CORROSION SCIENCE AND TECHNOLOGY, Vol.15, No.4(2016), pp.159~165 pISSN: 1598-6462 / eISSN: 2288-6524
DOI: http://dx.doi.org/10.14773/cst.2016.15.4.159

Influence of Retrogression and Re-aging on the Exfoliation Corrosion Behavior of AA 7085 Sheets

Ajay Krishnan[1], V. S. Raja[1,†], and A. K. Mukhopadhyay[2]

[1]*Department of Metallurgical Engineering & Materials Science, Indian Institute of Technology Bombay, Mumbai 400076, India*
[2]*Defence Metallurgical Research Laboratory, Hyderabad 500058, India*

(Received January 28, 2016; Revised July 04, 2016; Accepted July 05, 2016)

An attempt has been made to understand the influence of retrogression and re-aging (RRA) on the exfoliation corrosion behaviour of AA 7085 alloy in comparison with the peak aged condition (PA). Immersion tests using ASTM G34 and studies involving electrochemical impedance spectroscopy showed that the RRA treated alloy provided higher resistance to exfoliation corrosion than the PA treated alloy. The improved resistance was attributed to the enhanced Cu content and the discontinuous nature of the grain boundary precipitate, which was revealed through transmission electron microscopy.

Keywords : *aluminium alloy, exfoliation corrosion, impedance spectroscopy*

1. Introduction

High strength aluminum alloys are widely used for aircraft applications due to their high specific strength. These alloys are precipitation hardened and rely on fine precipitates for strengthening. Alloying elements which bring in heterogeneities to the material cause micro galvanic cells leading to pitting and intergranular corrosion. These could act as crack initiation sites leading to loss in structural integrity followed by catastrophic failures[1-3]. Exfoliation corrosion (EFC) is a form of intergranular corrosion which is prevalent among the cold worked 2xxx and 7xxx series aluminum alloys having a pan cake structure and occurs mainly due to grain boundary precipitates and associated grain boundary corrosion. The attack runs through grain boundaries parallel to the metal surface and subsequent lifting of grain takes place. This is called delamination. Generally it initiates from pits and leads to various forms of degradation such as flaking, powdering or formation of large blisters. The corrosion products which form have a larger volume than the original aluminium alloy and this exerts a wedging stress on the material that lift the surface grains[4]. Moreover, further research has proved that it can affect the stress corrosion property of the alloy. The sensitivity of an alloy to EFC can be controlled by an appropriate heat treatment although they cannot be completely suppressed. Robinson et al. showed that over aging the material reduces the intergranular corrosion susceptibility[5] whereas grain orientation and the degree of cold deformation also have an impact[6]. Frankel et al. showed that the grain boundary precipitates $MgZn_2$ play a crucial role for the EFC[7] and more recently more insights on the EFC behavior were reported through foil penetration technique under several conditions[8]. Traditional Cu rich 7xxx aluminum alloys such as AA7050, AA7150, AA7X49 and AA7055 have problems of high quench sensitivity. A recently developed AA7085 exhibits low quench sensitivity and is made possible for use as thicker alloy sections in aircraft[9,10] and it is considered for the present study as not much work has been published in this regard. The standard and widely used testing method for exfoliation corrosion is ASTM G34 EXCO test[11] termed as 'exfoliation corrosion' which uses a highly accelerated condition. The solution used for the study is called EXCO solution of pH 0.4 containing 4M of NaCl, 0.5M of KNO_3 and 0.1M of HNO_3 .However it is a qualitative representation based on the visual examination and fails to explain the extent of the EFC. Therefore a quantitative representation is required. Keddam et al. used EIS as a quantitative measurement technique to understand the EFC mechanism[12]. As EFC is a serious problem among the aircraft industry thereby understanding them is of prime interest. The aim of this work is to compare the EFC susceptibility of AA 7085 sheets in PA and RRA temper condition using EIS.

† Corresponding author: vsraja@iitb.ac.in

Table 1. Alloy composition

Element	Zn	Mg	Cu	Zr	Ti	Fe	Si	Al
Amount (wt. %)	7.5	1.24	1.2	0.14	0.096	0.04	0.04	Bal

Table 2. Summary of heat treatments

Heat treatment	Temperature Cycle	Designation
Peak aged (PA)	120 °C for 24 h	T6
Retrogression & Re-aging (RRA)	120 °C for 24 h+ 205 °C for 5 min + 120 °C for 24h	T77

2. Experimental Procedure

The material used in this study was AA 7085 received in the form of rolled sheets of 5 mm thickness from Defence Research Metallurgical Laboratory, Hyderabad, India. The composition of the alloy measured using inductively coupled plasma atomic emission spectroscopy technique (ICP- AES) is mentioned in the Table 1.

The material was subjected to two different heat treatments as mentioned in Table 2. A Solutionizing treatment at 455 ^{O} C for 1.5 h was given to all samples prior aging. Optical micrographs for both the heat treatments were taken in all the three directions prepared by the standard metallographic procedure and etched using Keller's reagent (95 ml water, 2.5 ml HNO_3, 1.5 ml HCl and 1 ml HF)

Transmission electron microscopy (TEM) was carried out to reveal the difference in grain boundary precipitates between the two aging conditions. Samples were dry polished to a thickness of 0.08 mm - 0.1 mm with a surface finish of 1200 grit SiC emery paper. From these thin sheets discs of 3 mm diameter was punched. The discs were thinned using ion milling with 4^{o} beam angle. The images obtained were taken on a JEOL 2100F field emission gun transmission electron microscope (FEG-TEM) at 200 kV. Potentiodynamic polarization and Electrochemical Impedance Spectroscoy (EIS) studies were carried out using a Biologic VSP potentiostat. All the tests were conducted with a three electrode setup; alloy being the working electrode, a platinum sheet as a counter electrode and a saturated calomel electrode as a reference electrode. Potentiodynamic polarization tests were carried out in freely exposed 3.5 wt.% NaCl at a scan rate 1 mVs^{-1} while the EIS studies were carried out in EXCO solution. Impedance studies were conducted at OCP and frequency ranged from100 kHz to 10 mHz with a sinusoidal voltage of amplitude ± 10 mV. The Biologic software (EC-Lab V10.17) was used for fitting and evaluation of the impedance data.

3. Results and Discussion

3.1 Optical micrographs

Typical micrographs for peak aged and retrogressed and re-aged samples are shown in Fig. 1 and 2 respectively Optical micrographs of both the heat treatments showed elongated grains along the long and short transverse directions which were a result of cross rolling and showcase a pancake structure. As evidenced, rolled surface showed

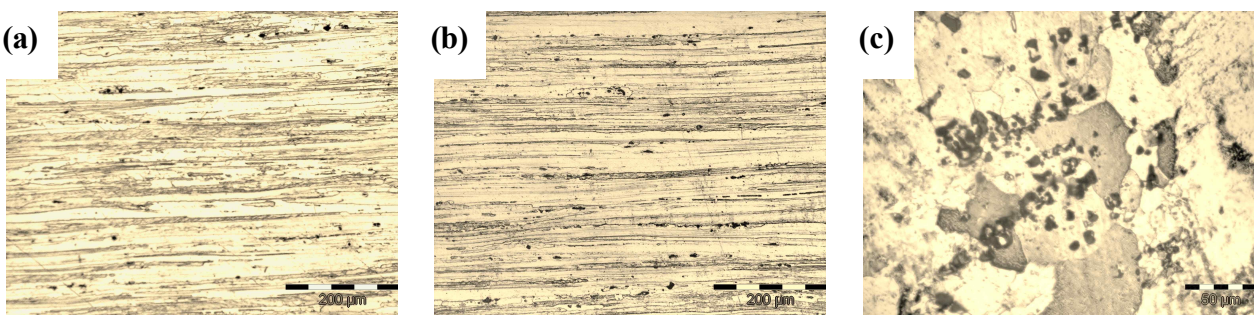

Fig. 1. Optical micrographs of peak aged specimens in all three directions. (a) Long transverse, (b) Short transverse, (c) Rolling direction.

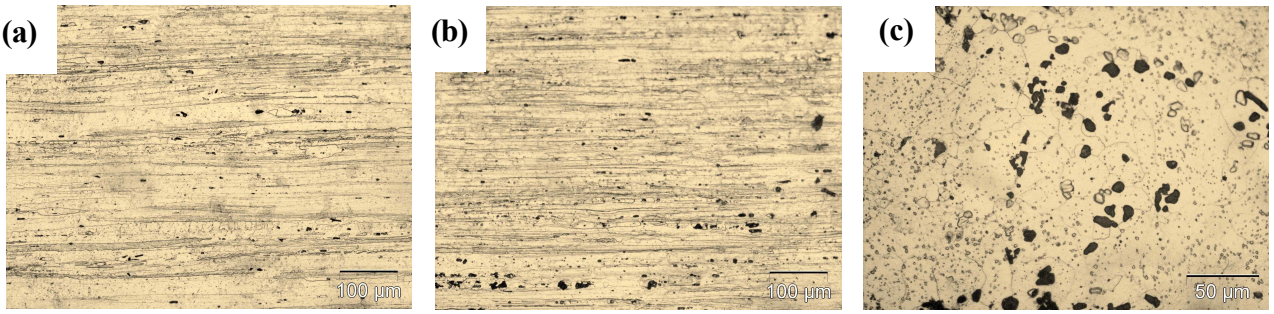

Fig. 2. Optical micrographs of retrogressed and re-aged specimens in all three directions. (a) Long transverse, (b) Short transverse, (c) Rolling direction.

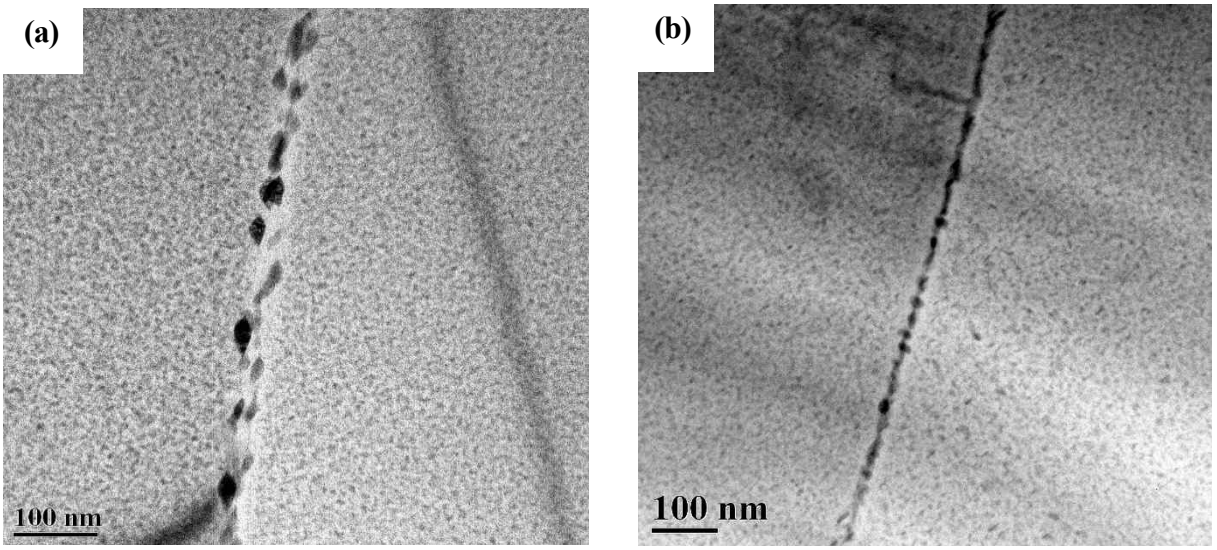

Fig. 3. Microstructural variations obtained after different heat treatments showing coarser and discontinuous network of grain boundary precipitates (a) retrogressed and re-aged and (b) peak aged.

recrystallized grains with some dark particles on it. These particles correspond to the coarse intermetallics which were formed during casting.

3.2 Transmission electron microscopy

Representative TEM micrographs for the peak aged and retrogressed and re-aged samples are shown in Fig. 3.

From the figure it is evident that the main difference between the heat treatments lies in the grain and grain boundary precipitate distribution. Peak aged sample showed a continuous distribution of η precipitates on the grain boundaries whereas RRA showed a relatively coarser and distant distribution of η precipitates on the grain boundaries. In addition, within the grains, the precipitates of the RRA temper were quite finer and denser than those of the peak aged temper. Further, the grain boundary precipitates of the peak and the RRA alloys showed 1.5 and 2.5 wt.% Cu respectively when measured using energy

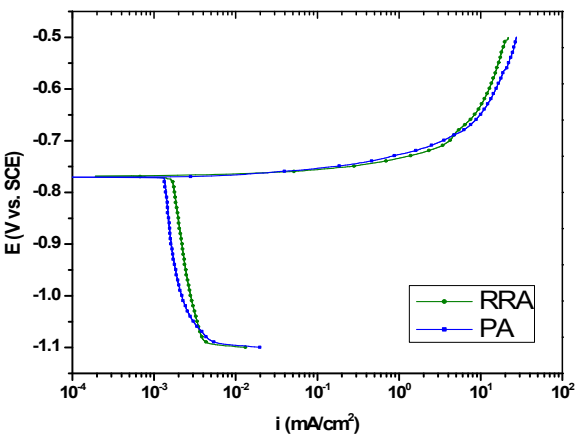

Fig. 4. Potentiodynamic polarization curves of AA 7085 in 3.5 wt.% NaCl after different heat treatments.

dispersive spectroscopy (EDS).

3.3 Potentiodynamic polarization

The potentiodynamic polarization curves of AA 7085 sheets under peak aged and retrogressed and re-aged condition obtained in 3.5 wt. % NaCl exposed freely in air are shown in Fig. 4.

The corrosion potential (E_{corr}) values of the retrogressed and re-aged (-768 mV) alloy is marginally nobler than that of peak aged (-775mV) alloy. The anodic currents increased very steeply above E_{corr} and examination of these curves clearly indicates the absence of passivity. Examination of these curves has indicated that the cathodic currents are almost independent of the applied potential. Because of the heterogeneities present in the material, the cathodic kinetics is accelerated and drives the E_{corr} towards more nobler potentials and this leads to pinning of E_{corr} with pitting potential (E_{pit})[13]. The cathodic currents under different heat treatments marginally increased in the order; peak aged< retrogressed and re-aged. Such increased cathodic currents were attributed to the increased oxygen reduction kinetics due to the Cu enrichment in the RRA condition.

3.4 Exfoliation corrosion

To examine the exfoliation corrosion behaviour of peak aged and retrogressed and re-aged alloys, samples were immersed in EXCO solution as per ASTM G34 and further quantified using EIS in freely exposed EXCO solution under different time intervals. EIS studies were carried out at 30 min, 3 h and 24 h exposure. Fig. 5 shows the Nyquist and Bode magnitude plots for the different time intervals. All the Nyquist plots are characterized by one capacitive loop whose radius kept decreasing over the time period of exposure. There is an evidence of inductive loop at low frequencies which disappeared after 24 h of immersion. The equivalent circuit having solution resistance (R_{sol}), constant phase element (Q_f) and a charge transfer resistance (R_f) was used to fit the impedance data, which excluded the data points corresponding to inductive behaviour. Considering the presence of micro structural heterogeneities in the alloys and the fact that the capacitive loop was a depressed semicircle, constant phase element Q_f was used for the electrochemical interface.

The data obtained from fitting the EIS plots are summarized in the Table 3.

The Nyquist plots of both the alloys showcased one capacitive loop with one time constant whose radius kept decreasing over the time of exposure. This is an indication that the process is under activation control. The pH of the solution was around 0.4 during the starting of the experiment and it kept increasing during the time period and reached a value of 3.2 after 24 h of immersion. The decrease in the arc radius of the capacitive loops was due to the aggressive chemical reaction that took place because of the EXCO solution. As the exposure time increased the surface became more heterogeneous and further dip in the arc radius was observed as reflected in the dip in the value of 'n'. However for 24 h immersion, the arc radius was higher than the 3 h immersion period. This could be because of the accumulation of corrosion product over the surface of the material which hindered further reaction.

3.5. Discussion

The 7xxx series aluminum alloys has a greater susceptibility to intergranular corrosion under the influence of chloride environment[14]. The grain boundary precipitates are Mg $(Zn,Al,Cu)_2$ complexes and are highly anodic in nature. These precipitates can undergo selective dissolution and exert a wedge force upon reaching a critical amount of corrosion products. Therefore, composition and the morphology of the grain boundary precipitates largely determine the intergranular resistance of these alloys. In the present study, retrogression and re-aging temper has been shown to exert better exfoliation corrosion resistance than the conventional peak aged temper. The visual examination after different time intervals of EFC tests in accordance with ASTM G34 are mentioned in the Fig. 6.

Table 3. Summary of EIS data

State of the sample	$R_{sol(\Omega.cm^2)}$			Q_f (μFcm^{-2})			n_f			$R_{ct}(\Omega.cm^2)$		
	30 min	3 h	24 h	30 min	3 h	24 h	30 min	3 h	24 h	30 min	3 h	24 h
PA	2.17	2.17	1.85	112.9	998.7	1848	0.8	0.7	0.7	55.5	11.78	20.86
RRA	2.10	1.95	1.84	531.2	2598	4982	0.7	0.7	0.6	28.65	7.94	15.72

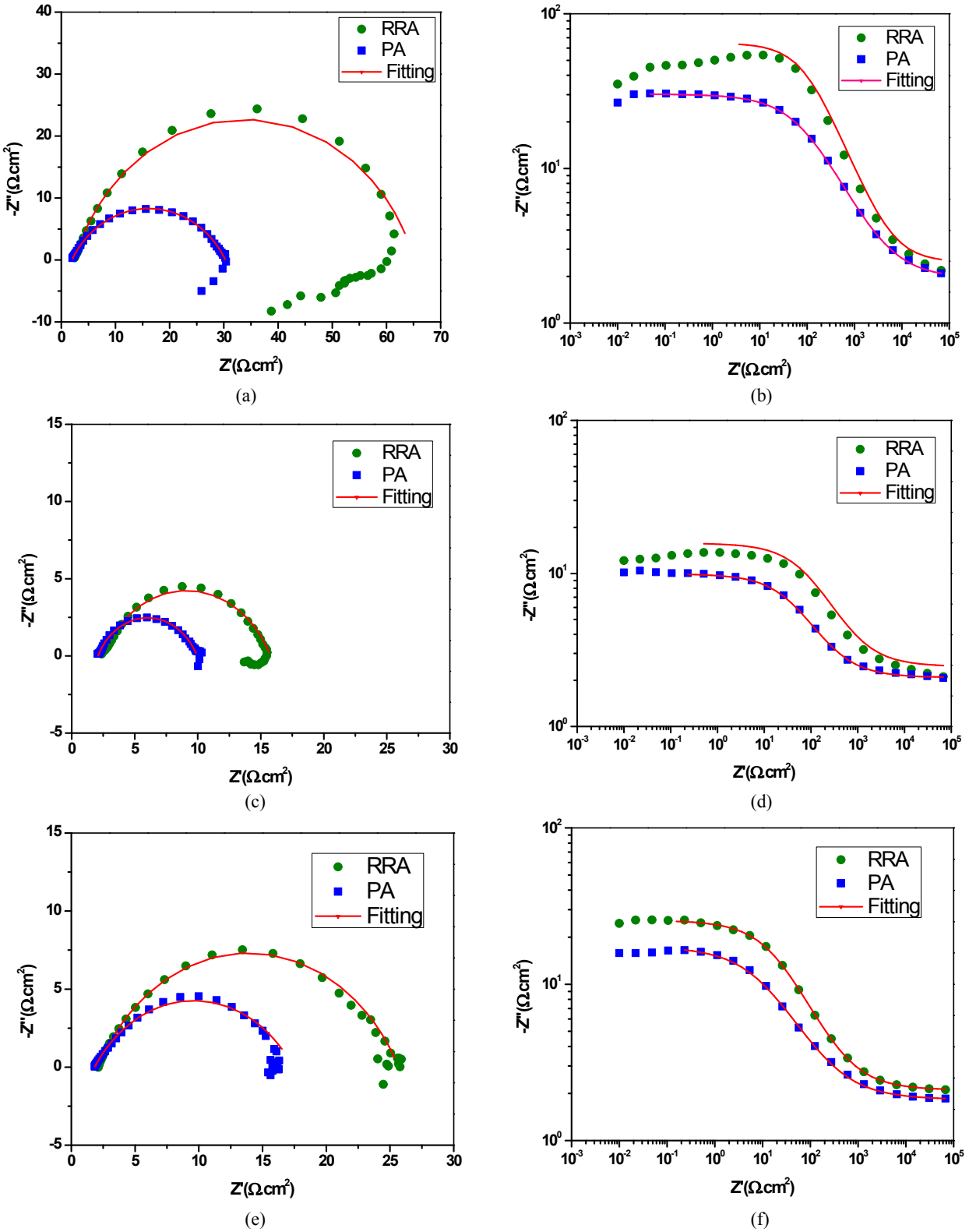

Fig. 5. Nyquist and Bode |Z| plots of RRA and PA alloys for various exposure times. (a) & (b): 30 min of immersion, (c) & (d): 3 h of immersion, (e) & (f): 24 h of immersion.

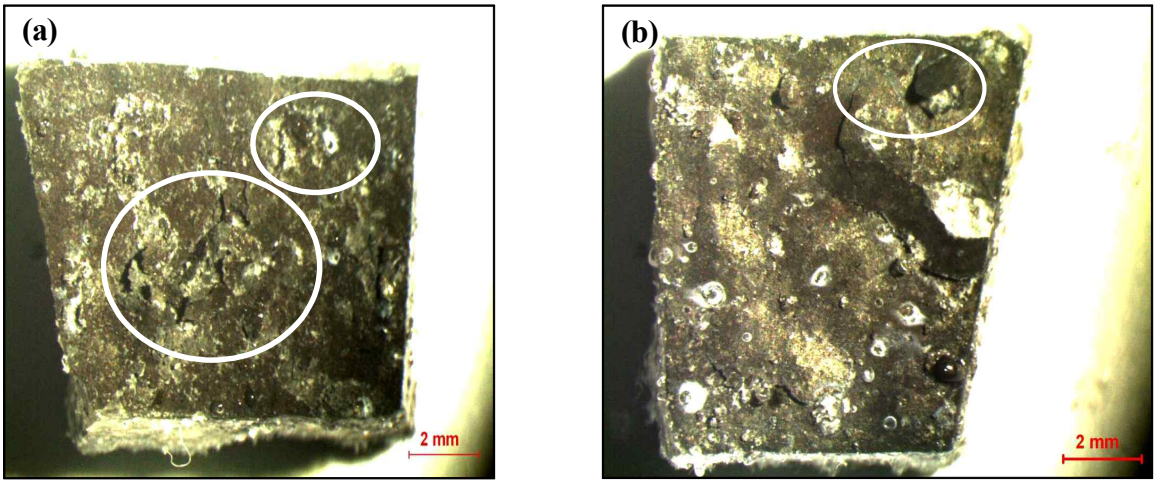

Fig. 6a. Stereo Macrographs of samples immersed in EXCO solution after 24h showing blisters on the surface (a) peak aged (b) retrogressed and re-aged.

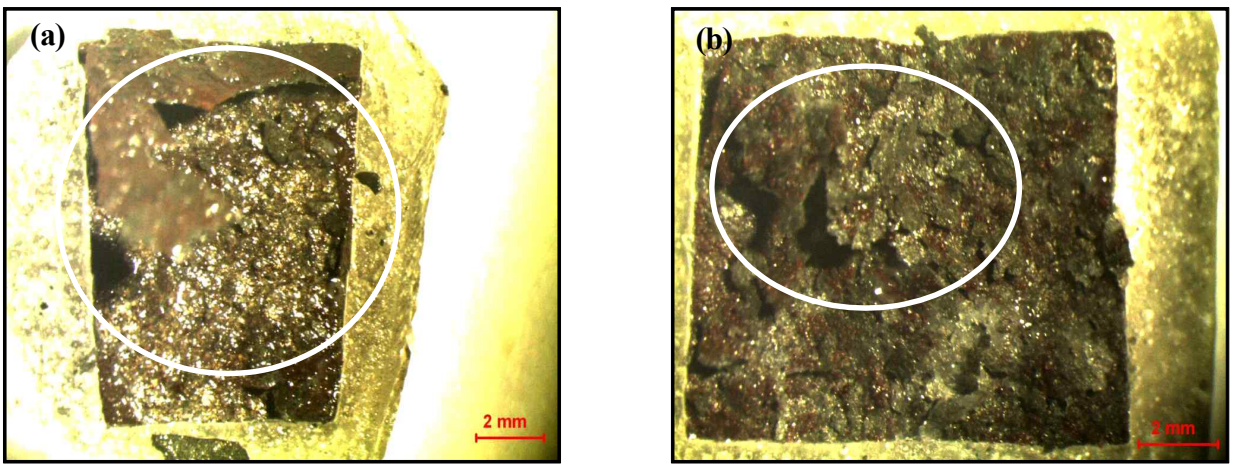

Fig. 6b. Stereo Macrographs of samples immersed in EXCO solution after 48h showing delaminated layers (a) peak aged (b) retrogressed and re-aged.

It is very evident from these macrographs that the peak aged alloy has suffered extensive delamination after 48h of immersion. On the contrary, the RRA alloy has few signs of delamination indicating that they are resistant to exfoliation corrosion. In terms of rating, RRA alloy has been rated to EB and peak aged alloy to ED indicating their lower exfoliation resistance. However, these ratings according to ASTM G34 are highly qualitative in nature. In order to quantify them, the alloys were subjected to EIS studies for different time intervals. The Nyquist plots of PA alloy showed one inductive loop whereas RRA alloy showed two at low frequencies which disappeared after 24 h of immersion. It can be related to anodic dissolution activity which is more promising at a pH of 0.4. In addition, the higher anodic nature of the grain boundary precipitate with lesser Cu on the grain boundary precipitates supports this data. Conde et al. suggested the appearance of this pseudo inductive arc to the slow changes in the system chemistry or the adsorption of chlorides[15] while Keddam et al. mentioned that the inductive arc may occur because of the weakening of the protective aluminum oxide layer due to severe anodic dissolution[12]. The authors believe the enhanced Cu content might have played a role in retarding the anodic dissolution of these precipitates. At a pH of 0.4 the reaction would be very aggressive leading to the weakening of the protective oxide film. Another observation is about the increment in the double layer capacitance and decrease in the charge transfer resistance over the time of exposure. Mansfeld et al.[16-18] reported that reduction in the height and width

of the maximum of the phase angle is related to the decrease in the charge transfer resistance (R_{ct}) and increase in the double layer capacitance (Q_f). This has been observed by the authors and mentioned in the Table 3. However the plots for the same are not shown here.

As evident from the TEM micrographs, the remarkable resistance of RRA alloy lies in the distribution of the η precipitate along the grain boundary and its associated chemistry. Various researchers have shown that[19-22] a change in temper condition can change the Cu content along the grain boundary precipitates and adversely affect the intergranular corrosion resistance. RRA alloy has more Cu in the grain boundaries than the PA alloy. The higher temperature aging in the RRA seems to have increased the copper content on the grain boundary precipitates[23] This will change the anodic nature of the precipitate to a relatively nobler state that that of in PA alloy and thereby reducing the intergranular corrosion. The EXCO test data and the EIS data show the fact that RRA treated alloy perform better than the PA temper in aggressive corrosive conditions.

4. Conclusions

The study has led to the following conclusions.

1. RRA treated alloy showed better exfoliation resistance than the PA alloy in EXCO test supplemented by the EIS studies.
2. Both the heat treatments exhibited one capacitive loop whose arc radius decreased along the course of the experiment. The RRA alloy showed a relatively coarser and discontinuous distribution of grain boundary precipitates while the PA alloy showed a continuous distribution of grain boundary precipitates.
3. Semi quantitative measurement of grain boundary precipitates revealed more Cu in RRA alloy than PA which made the η precipitates relatively nobler and improved the intergranular corrosion resistance.

Acknowledgement

The authors would like thank Defence Metallurgical Research Laboratory for funding this project under CARS scheme.

References

1. T. -S. Huang and G. S. Frankel, *Corros. Sci.*, **49**, 858 (2007).
2. J. P. Chubb, T. A. Morad, B. S. Hockenhull and J. W. Bristow, *Int. J. Fatigue*, **17**, 49 (1995).
3. M. Liao, G. Renaud and N. C. Bellinger, *Int. J. Fatigue*, **29**, 677 (2007).
4. D. McNaughtan, M. Worsfold and M. J. Robinson, *Corros. Sci.*, **45**, 2377 (2003).
5. M. J. Robinson and N. C. Jackson, *Corros. Sci.*, **41**, 1013 (1999).
6. J. Wloka, T. Hack and S. Virtanen, *Corros. Sci.*, **49**, 1437 (2007).
7. T. Ramgopal, P. Schmutz and G. S. Frankel, *J. Electrochem. Soc.*, **148**, B348 (2001).
8. T. -S. Huang and G. S. Frankel, Corrosion, **63**, 731 (2007).
9. C. Li, Z. Chen, S. Zeng, N. Cheng, Q. Li and Z. Geng, *Adv. Mat. Re.*, **228-229**, 968 (2011).
10. S. Liu, Q. Zhong, Y. Zhang, W. Liu, X, Zhang, Y. Deng, *Materials & Design*, **31**, 3116 (2010).
11. ASTM-G34, Standard Test Method for Exfoliation Corrosion Susceptibility in 2XXX and 7XXX Series Aluminum Alloys (EXCO Test) 1, ASTM. 01, 1 (2013).
12. M. Keddam, C. Kuntz, H. Takenouti, D. Schuster and D. Zuil, *Electrochim. Acta*, **42**, 87 (1997).
13. M. B. Kannan, and V. S. Raja, *Metall. Mater. Trans. A*, **38**, 2843 (2007).
14. T. D. Burleigh, *Corrosion*, **47**, 89 (1991).
15. A. Conde and J. de Damborenea, *Electrochim. Acta*, **43**, 849 (1998).
16. F. Mansfeld, *Electrochem. Acta*, **35**, 1533 (1990).
17. F. Mansfeld, *Electrochem. Acta*, **38**, 1891 (1993).
18. F. Mansfeld, *J. Appl. Electrochem.*, **25**, 187 (1995).
19. A. K. Mukhopadhyay, K. S. Prasad, V. Kumar, G. M. Reddy, S. V. Kamat and V. K.Varma, *Mater. Sci. Forum*, **519**, 315 (2006).
20. A. K. Mukhopadhyay, *T. Indian I. Metals*, **62**, 113 (2009).
21. M. A. Krishnan, V. S. Raja, *Corros. Sci.*, **109**, 94 (2016).
22. M. Bobby Kannan, R. Raman, A. Mukhopadhyay, V. S. Raja, *Corrosion*, **59**, 881 (2003).
23. T. Marlaud, A. Deschamps, F. Bley, W. Lefebvre and B. Baroux, *Acta Mater.*, **58**, 4814 (2010).